LEGIBILITY NOTICE

A major purpose of the Technical Information Center is to provide the broadest dissemination possible of information contained in DOE's Research and Development Reports to business, industry, the academic community, and federal, state and local governments.

Although a small portion of this report is not reproducible, it is being made available to expedite the availability of information on the research discussed herein.

LA-UR -88-1168

CONF-880844--2

LA-UR--88-1168

DE88 009157

TITLE THE INFLUENCE OF TEXTURE ON STRAIN HARDENING

AUTHOR(S) U. F. Kocks, CMS
M. G. Stout, MST-5
A. D. Rollet, MST-6

SUBMITTED TO Talk to be given at the 8th International Conference on the Strength of Metals and Alloys (ICSMA) at Tampere, Finland on August 22-26, 1988.(INVITED PAPER)
To be published by Peragon Press.

Los Alamos Los Alamos National Laboratory
Los Alamos, New Mexico 87545

THE INFLUENCE OF TEXTURE ON STRAIN HARDENING†

U. F. Kocks, M. G. Stout, and A. D. Rollett

Los Alamos National Laboratory
Mail Stop K-765, Los Alamos NM 87545, USA

It is well known that the strain hardening behavior of metals is not the same in tension, compression, torsion and rolling, for example. The comparison is usually made on a basis of vonMises equivalent stress and strain. One reason for this difference lies in the development of deformation textures, which depends on the straining path. We report on a new set of experiments, comprising wire-drawing interrupted by tensile tests, free compression, channel-die compression, and short-tube torsion in aluminum, an Al-Mg alloy, copper, silver, and 70:30 brass. The texture was measured before straining and at vonMises strain levels of roughly 1.0 and 2.0. Computer simulations of the deformation, starting from a set of random grains weighted by the observed initial texture, predicted deformation textures in qualitative agreement with the observed ones in most cases. Quantitatively the simulations yielded the Taylor factors as a function of strain for all paths and, with an assumed hardening law for the representative grain, the macroscopic stress/strain curves The grain hardening rate as a function of resolved shear stress was described in tabular form such as to match one of the macroscopic curves, and then used to predict the others. The eventual fit was quite good; we will describe what judgments needed to be made to achieve this result. The conclusion is that the strain-path dependence of work hardening can be explained simply as a consequence of texture development.

KEYWORDS: strain hardening, multi-axial, texture, experiment, simulation

---

† Work supported by the U.S. Department of Energy, Basic Energy Sciences.

INTRODUCTION

It is generally recognized, but also generally ignored, that the stress strain curve of engineering materials is controlled by at least two factors: intrinsic strain hardening by dislocation accumulation, and changes in the texture of the polycrystals. For completeness, we should mention the third major component: the accumulation of macroscopic internal stresses, especially in two-phase alloys and composites. The two 'physical' mechanisms, dislocations and internal stresses, have drawn much attention. The former is the most basic, but is conceded to be a difficult topic to treat quantitatively, for macroscopic averages. By contrast, macroscopic hardening (and softening) due to texture changes, being entirely geometrical in nature, can be treated quantitatively with much more confidence, but this capability has not been extensively applied to cases of technical interest.

Texture effects are particularly important in multi-axial stress/strain behavior. Obviously, the yield stresses in tension in different directions need not be the same in anisotropic materials. Furthermore, the yield stresses in uniaxial deformation and in shear, which are in general different even for isotropic materials, may be considerably more different from each other in textured materials. Finally, and most crucially, the rate of hardening along different straining paths, such as tension, compression, rolling, and torsion, depends on the different grain rotations in the different cases. In a previous paper, these effects were shown to be substantial (Tomé and co-workers, 1984). The present work presents further developments in a quantitative assessment.

The basis for this assessment is two-fold: first, a new set of experiments on multi-axial strain hardening; and second, a rather mature and versatile program for computer simulation of polycrystal plasticity. With respect to experiments along different straining paths, one must watch out for extraneous effects: the friction and other boundary conditions tend to be different; the strain rate is often markedly different; and finally, the materials are often only nominally the same but may, for example, have different initial textures for the different tests. The set of experiments to be reported here have taken account of all these effects with particular care. In addition, textures were measured both before and during the tests. A variety of different materials was used: all single-phase metals of face-centered cubic lattice structure.

The simulations were undertaken with the Los Alamos Polycrystal Plasticity (LApp) code. Each of a set of 800 randomly oriented grains was weighted with the measured initial texture for each material separately and then deformed, under 'relaxed' uniform straining conditions, along the various straining paths. A hardening law for the representative grain was chosen such as to match one of the experimental polycrystal stress/strain curves for this material, and was then used to predict the others stress/strain curves. The general conclusion will be that all of the experimentally observed differences for different straining paths *can* be explained on the basis of texture differences alone: if anything, the simulations tend to overexplain the effects.

EXPERIMENTAL PROCEDURES

Five materials were tested: 1100 aluminum and an Al-2%Mg alloy; OFE copper and 70:30 brass (lead-free); and 99.9% pure silver. The sample preparation generally involved cycles of swaging (or, in the case of copper, rolling) and recrystallization. The recrystallization anneals after final machining were as follows: brass and silver 450°C 1/2 hr, copper 600°C 1 hr, aluminum 343°C 1/2 hr, and Al-Mg 380°C 1 hr. These heat treatments resulted in a 40 μm grain size, except 40 μm in silver, and 100 μm in Al-Mg. The grain shapes were generally slightly elongated in the direction of the subsequent deformation axis; the most extreme case was aluminum, where the aspect ratio was 1.5

The five materials were deformed by wiredrawing, compression, and torsion to von Mises equivalent strains of 0.87 and 2.04 (for the brass, 1.08 and 1.89). In addition, a tensile test was undertaken for the Cu, and a channel-die test for the Al-Mg alloy. A strain rate of $\sim 10^{-3}$ s^{-1} was maintained, in the average, for all experiments.

Cylinders for wiredrawing were initially 15.9 mm in diameter. Drawing was through dies with a 16° included angle giving a 0.288 reduction of area. The low-angle large reductions were to minimize redundant work. "Molykote" spray was used for lubrication in the drawing. The compression experiments began with cylinders 12.7 × 12.7 mm. After deformation increments of 0.25, the cylinders were remachined to a diameter of 12.7 mm. After each increment, the samples were relubricated with various combinations of Teflon and molybdenum disulfide; the final recommended procedure was to use 0.003" thick cast Teflon tape with Molycote spray on the interface between it and the specimen only. The same lubrication procedure was used on channel-die compression; here, the initial specimen dimensions were 14 × 10 × 7 mm, and the channel width was reduced from 10 to 7 to 5 mm as the specimen was spark-cut and planed to successivly smaller dimensions of about the same initial aspect ratios. Torsion was done using a short thin-walled tube: 16.7 mm OD, 15.2 mm ID, gauge length 3.2 mm.

The problems of interpretation are different for the different tests. While wiredrawing itself requires more work than a tensile test, the tensile tests that were used after various amounts of wiredrawing provide a lower bound on the current flow stress because the specimens neck immediately. In compression and in the channel die, the uncertain factor is friction; its influence is deemed negligible because the specimens did not barrel, and reloading after relubrication produced a good continuation of the stress strain curve. The torsion of short tubes has the advantage over long tubes that buckling does not occur at large strains; but the disadvantage that the strain measurements are not as precise.

Pole figures for {111}, {200}, and {220} were measured with an automated pole figure device using a copper $K\alpha$ radiation operating at 40 kV and 20mA. Both angles were increased from 0° in 5° steps to 80° and 355° respectively, usually counting for 1 s at each step. Both background and defocussing corrections were applied from measured data on random samples of each material (Wenk, 1985). Where complete orientation information was needed (for the initial textures, and to obtain inverse pole figures), it was obtained using a WIMV algorithm (Matthies and Wenk, 1985; Kallend, 1987). The recalculated pole figures agreed with the measured ones to an RP-error (Matthies and Wenk, 1985) of about 0.05.

EXPERIMENTAL RESULTS AND QUALITATIVE EXPLANATION

Figure 1 displays most of the stress/strain results. The behavior of the Al-2%Mg alloy (right top) is a mechanical engineer's dream: when you plot wire-drawing, compression, and torsion data on the basis of von Mises equivalent stress and strain, all curves fall together, to an acceptable approximation. We also obtained data on channel-die compression, an idealization of sheet rolling; they were only taken to a strain of 0.4 (because shear banding intervened) and are not displayed, but they fell on the same curve also. We shall see that this 'ideal' behavior is unexpected. In fact, we found upon re-checking our data that the torsion tests were done from a different batch of alloy: when we repeated compression tests for that alloy, they fell considerably above those shown here; thus, the torsion curve to be compared with the other data in this figure should be lower.

The 1100 aluminum (left top) shows one of the 'typical' behaviors: while all the stress/strain curves look qualitatively the same, the torsion curve is at a level about 20% lower than the wire-drawing and compression data. This difference is too much to be possible for isotropic materials under *any* assumed yield function: it must be due to anisotropy. (These test specimens were taken from the same block of material: note that "1100 aluminum" is quite a variable material.) In fact, the anisotropy is in the expected direction: this test material was prepared by swaging and recrystallization, and the ensuing texture is always a pronounced <111> fiber texture. In the case of this aluminum, it was a very strong initial texture of this kind (Fig. 2a). Now <111> is known to have the highest of all Taylor factors for tension and compression, but one of the lowest for torsion. If the fiber texture were ideally sharp, the ratio of the initial flow stresses in compression and torsion should be about 1.8: the fact that it is only 1.2 is a consequence of the dispersion of the fiber texture.

The case of copper displays another kind of 'typical' behavior: while the stress/strain curves are fairly close together at the beginning (reflecting the fact that the initial texture was weaker), they diverge at large strains. Note that this is true even in a comparison of wiredrawing and compression. In this case, an initial curve for true tension is also shown: the wiredrawing-plus-tension data fall nicely on the extension of the tensile curve. The increasing divergence of the curves at large strains can be explained qualitatively on the basis of changing Taylor factors for different strain paths (Fig. 3).

The behavior of silver was similar to that of copper. (We did not have wire-drawing data at the time of this writing.)

Finally, the brass displays an extreme case of divergence at larger strains. A qualitative explanation for this observation follows immediately from the fact that the initial texture for this material was the weakest (Fig. 2b): thus, the von Mises equivalent stress is a reasonable approximation at yield but, on the other hand, the subsequent development of Taylor factors is greater here than in the other cases. A quantitative explanation is hampered by the fact that the compression texture (Fig. 2d) is here not in accord with predictions (which yield something similar to the case of compressed Al, Fig. 2c). This is presumably due to the fact that deformation twinning was ignored in our simulations but was especially copious in brass.

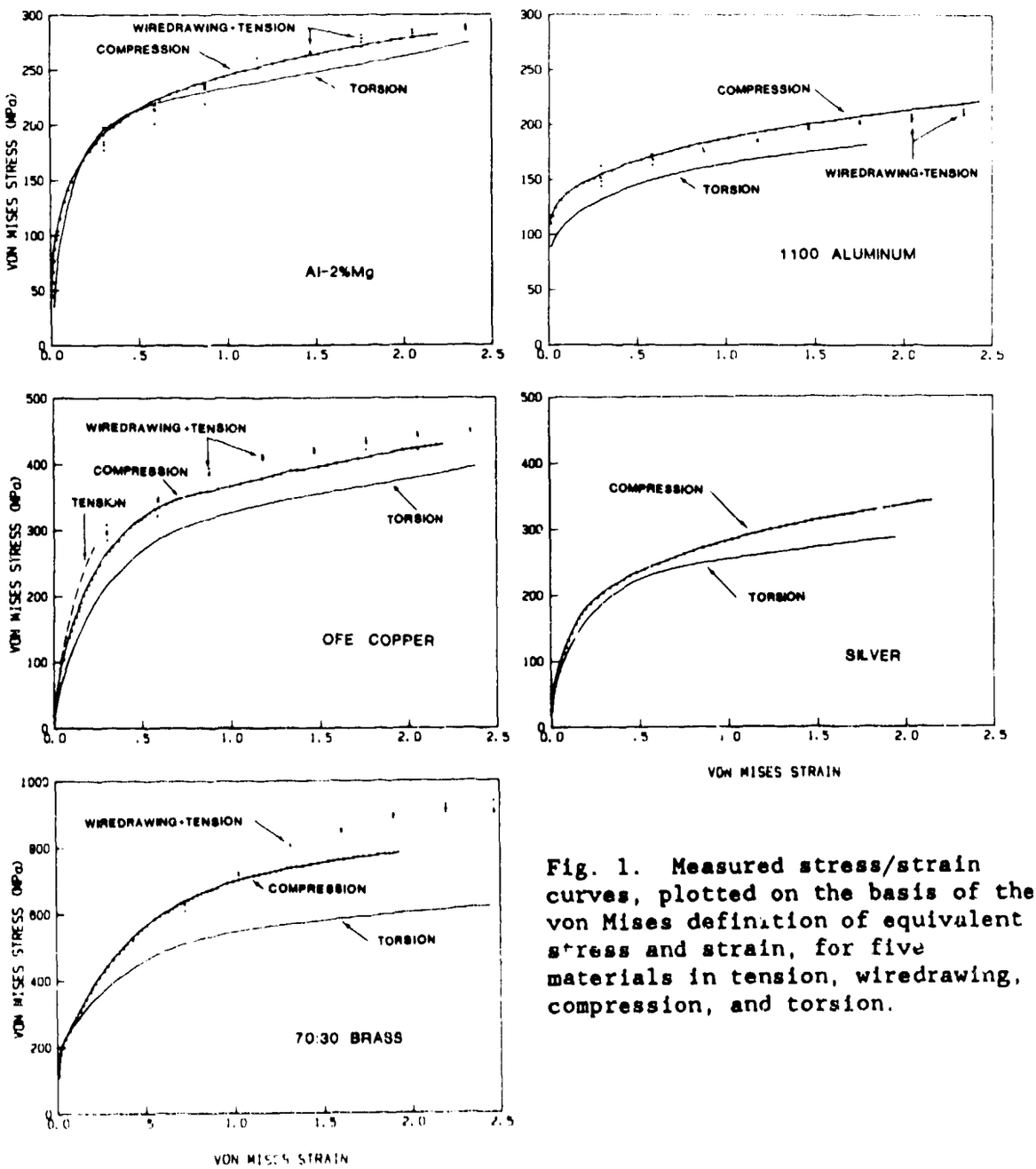

Fig. 1. Measured stress/strain curves, plotted on the basis of the von Mises definition of equivalent stress and strain, for five materials in tension, wiredrawing, compression, and torsion.

DESCRIPTION OF HARDENING

A simple way to analyze the measured stress/strain curves would be to use average Taylor factors $\langle M \rangle$ derived from simulation (such as those for Cu, shown in Fig. 3) to obtain the underlying average curve of resolved shear stress versus resolved shear for each case. In general, this may give rise to different grain stress/strain curves for each strain path, which would then indicate a dependence of intrinsic hardening on strain path. This procedure was used in the previous paper (Tomé and co-workers, 1984), and it was pointed out that the averaging over polycrystal properties is not done correctly this way (even though the effect was shown to be negligible in that case). There is, however, a more fundamental drawback to this procedure: it does not lend itself to *predictions*.

In the present work, we have assumed that a unique grain hardening law exists. While it cannot be measured independently, because of the complicated effects of multiple slip (Kocks, 1970) and grain-boundary influences (Mecking, 1981), it can be obtained by an iterative procedure. We base it on a differential description; i.e. that the strain-hardening rate θ is a function of the resolved stress τ. A way to start is with a Voce law:

$$\theta/\theta_0 = 1 - (\tau - \tau_0)/\tau_v \qquad (1)$$

This serves to define three material constants: the resolved stress τ_0 and hardening rate θ_0 at yield; and the rate of decrease of θ with τ, characterized by the Voce stress τ_v. The Voce law is never strictly obeyed over the entire range of strains, but it could be used in some average sense; we found this to be too inaccurate to be useful in the present context.

What we have done instead is to use the Voce law to describe limiting behavior at low stresses, but describe the $\theta(\tau)$ law in tabular form (amounting in fact to a piecewise linear stress/strain law) so it can be modified at large strains to fit the actual behavior for each material. Figure 4 shows the results for three materials: they look quite similar to each other and to the Voce law (the straight-line decay), but the deviations at large values of τ give rise to very substantial differences in the stress/strain behavior. The value of τ_v is then to be looked upon as a stress-scaling parameter (Mecking and co-workers, 1986), but loses any semblance of a 'saturation' stress. It is well-defined even from the smallish strains achievable in tension (which are still the most reliable tests available). Also, θ_0 retains the quality of being very insensitive to material, temperature, and other variables.

Once a grain hardening law $\theta(\tau)$ is given, the macroscopic behavior follows, now with exact averaging, according to

$$\Delta\sigma = \langle M^2 \, \theta(\tau) \rangle \, \Delta\varepsilon \qquad (2)$$

where the Taylor assumption $\Delta\varepsilon$ = constant was used for the components of $\Delta\varepsilon$ that do work (and the change of M with ε during one step was neglected). Finally, we have used Taylor's assumption of isotropic hardening within the grains, according to

$$\Delta\tau = \theta(\tau) \, M \, \Delta\varepsilon \qquad (3)$$

The implications of this assumption, and its relative acceptability, are discussed in a recent paper (Kocks and co-workers, 1988).

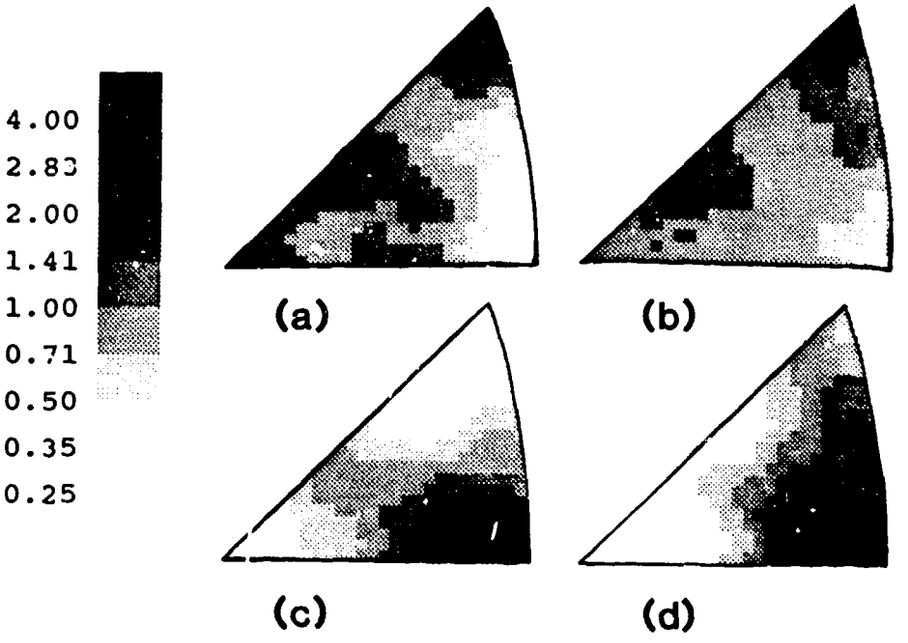

Fig. 2. The experimental textures before (a,b) and after (c,d) compression to a strain of 0.9, for aluminum (a,c) and brass (b,d). Inverse pole figures after WIMV conversion.

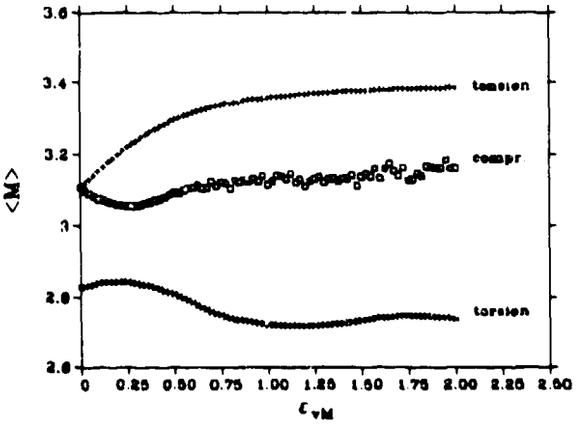

Fig. 3. Average Taylor factors as a function of strain, as calculated for the initial texture observed in copper.

POLYCRYSTAL SIMULATIONS

It is generally conceded that among simple assumptions the one due to Taylor, with its emphasis on compatibility over equilibrium considerations, is most appropriate for large-strain plasticity (Kocks, 1970). The various modifications that have been suggested were recently tested with respect to their influence on the predicted textures (Kocks, 1987). Only one of these modifications was found to be crucial: the influence of grain shape on a relaxation of constraints, and thus on the number of required slip systems (Honneff and Mecking, 1978; Kocks and Chandra, 1982; Kocks and Canova, 1981). In the current context, this is important for compression and torsion, but not for tension and wiredrawing (which was treated erroneously in Kocks and Canova, 1981). The method by which the developing flatness of grains is quantitatively used to increase the degree of relaxation of constraints has so far been based on plausible assumptions only; it may have to be modified so that its influence on macroscopic stress/strain curves matches observed behavior.

The predicted textures are generally in good qualitative agreement with observations, and there is little indication that they depend on the specific material (Stout and co-workers, 1987). The major quantitative deviation is that all predicted textures are too sharp. It was therefore anticipated that, for the purpose of describing and predicting hardening behavior, we would have to artificially slow down the rate of orientation changes. To our surprise, there was not sufficient evidence from our measured deformation textures to warrant such a procedure: we have taken the geometry of slip at face value.

Most texture simulations in the past were done assuming initial isotropy. In the current context, it is crucial that the actual initial textures are used as a starting point. For this purpose, the orientation distribution that was obtained from the measured initial textures was used to assign weights to a set of 800 random grains (Kallend, 1987). These weights are accounted for in the averaging processes in the code.

All simulations were done using the Los Alamos Polycrystal Plasticity (LApp) code, on a CRAY-XMP48, in about 3 CPU-seconds per strain step. The stresses were determined on the basis of a Bishop-Hill procedure, using the properties of the single-crystal yield surface. The distribution of slips was obtained by using a very small power-law rate sensitivity in a Newton-Raphson scheme.

On this basis, we have done a detailed analysis for the three commercially 'pure' materials. Using the grain hardening laws in Fig. 4, we obtained the macroscopic stress/strain curves displayed in Fig. 5. A general inspection shows very satisfactory agreement with the measured curves in Fig. 1.

To explain the details, let us start with copper. Here, the tensile curve was used to establish the three Voce parameters. (They are shown, for all three materials, in Table 1.) Using these results to predict compression at low strains (where full constraints apply) gave perfect agreement with the experiments. Then, the rest of the compression curve and the wire-drawing data were used to establish the points on the $\theta(\tau)$ table (Fig. 4) at large values of τ/τ_v. Using our established scheme to assess the degree of relaxation of constraints would have led to too much of a difference between the compression and wiredrawing data. Treating compression under full constraints would have led to too little a difference. Thus we decided to incorporate relaxed constraints at 1/4 the rate previously used: this is what led to the curves shown for Cu in Fig. 5. Applying the same criteria and the same $\theta(\tau)$ table to predict the torsion curve would have made it come out too low. The curve shown was obtained by assuming full constraints for torsion.

In summary for copper, we have the following situation. Applying the code before making any 'fits' would overpredict all the differences for the different strain paths. In principle, this could be due to a dependence of intrinsic strain-hardening behavior on strain path; but it would have to be *greater* in torsion than in uniaxial deformation, and it would have to different for tension and compression: both quite unlikely scenarios. The code has, it seems to us, only one major uncertainty built in: the rate of relaxation of constraints. Using this to fit the observations required different assumptions for compression and torsion; we cannot explain why.

At this point, the *same* assumptions were used for aluminum and silver – and the results were equally satisfactory. In fact, one could call the agreement quantitative in these two cases. In copper, there was one further

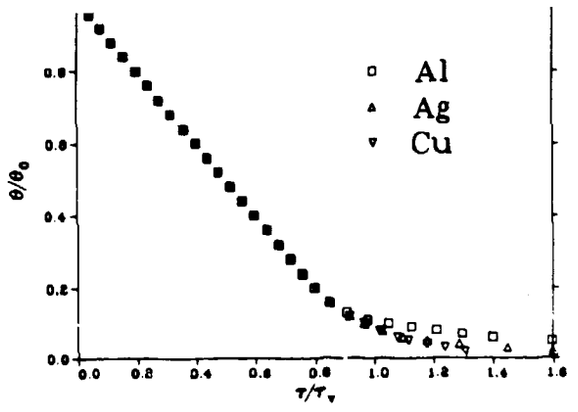

Fig. 4. The rate of strain hardening at the grain level, θ, as a function of the resolved shear stress, τ, both normalized by scaling parameters.

TABLE 1
Voce hardening parameters, all in MPa.

Material	τ_0	θ_0	τ_v
1100 Al	35	50	14
OFE Cu	10	210	90
Ag	18	106	60

Fig. 5. Results of simulation by the LApp code, for the initial textures and the hardening laws obtained for the three different materials. To be compared with the experiments in Fig. 1.

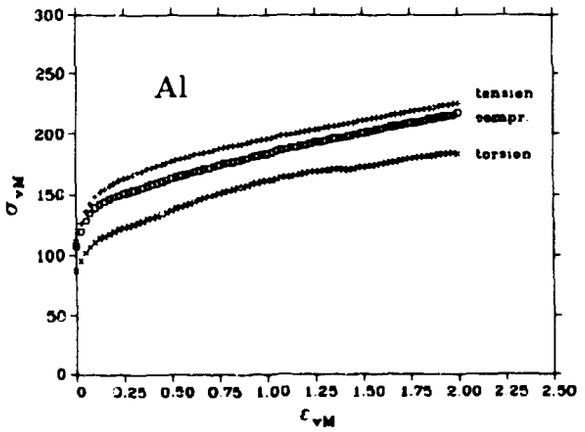

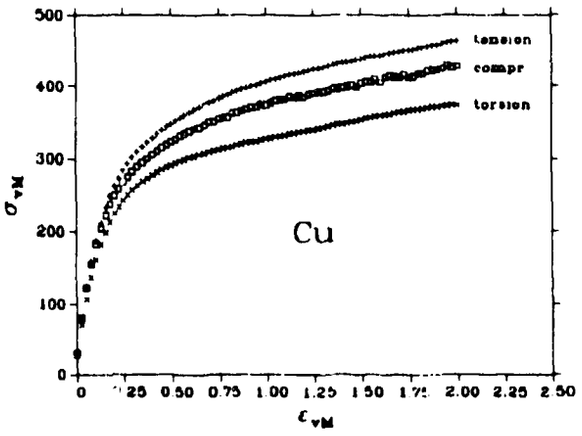

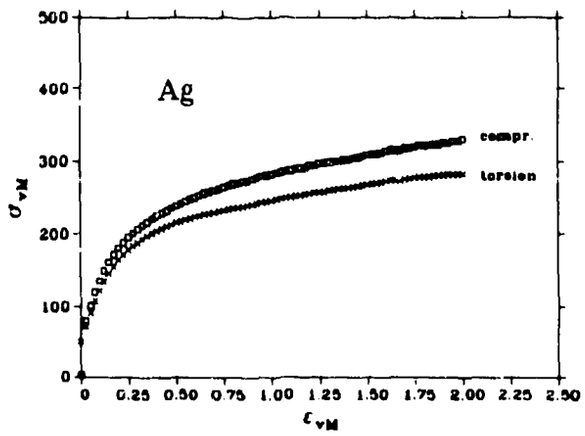

difficulty not mentioned before: the torsion curve at low strains could not be made to agree with the experimental one. We surmise that the strain measurements in this case may have been unusually inaccurate, because the low yield and high initial work hardening combine to cause significant deformation in the grips.

CONCLUSIONS

1. The differences between stress/strain curves under different straining conditions are often due to slight differences in material, in particular to different initial textures.

2. For the same material and initial texture, the different influences of this texture on the flow stress under different straining conditions, and the different development of the texture for different paths, can easily explain all the macroscopically observed behavior. In fact, since the tendency is for the texture effects by themselves to overpredict the differences, it is unlikely that potential differences in intrinsic hardening for different strain paths are significant.

3. The major uncertainty in present polycrystal simulation codes is the quantitative way in which the constraints are increasingly relaxed with progressing flatness of the grains; it is not uncertain that this effect must be taken account of. We found a way to adjust the code to fit all curves for copper, and then correctly predict the differences between compression and torsion for aluminum and silver.

4. A method is prescribed for assessing the intrinsic grain hardening law from experimental data on polycrystals. The small-strain behavior, which can be accurately measured, and can be evaluated without any influence of relaxed constraints, is decribed by a Voce law, using three parameters for each material. The large-strain behavior must be assessed in an iterative procedure, and described in tabular rather than equation form.

ACKNOWLEDGMENTS

The authors appreciate the skillful help with the experiments provided by M. L. Lovato, J. F. Bingert, and D. E. Nye. The pole figure measurement and evaluation procedure was based on the expert collaboration of H.-R. Wenk and J.S. Kallend. The LApp code was developed in intensive collaboration with G.R. Canova and C. Tomé. Finacial support for this work has been provided by the U.S. Department of Energy, Office of Basic Energy Sciences.

REFERENCES

Honneff, H., and H. Mecking (1978). In G. Gottstein and K. Lücke (Eds.), *Textures of Materials*. Springer. pp. 265-275.

Kallend, J.S. (1987). Unpublished. Illinois Inst. of Technology, Chicago.

Kocks, U.F. (1970). *Metall. Trans.*, 1, 1121-1143.

Kocks, U.F. (1987). In J.S. Kallend and G. Gottstein (Eds.), *Int'l. Conf. on Textures of Materials*. The Metallurgical Society, Warrendale, Pa. In press.

Kocks, U.F., and G.R. Canova (1981). In N. Hansen et.al.(Eds.), *Deformation of Polycrystals*. Risø National Laboratory, Roskilde, Denmark. pp.35-44.

Kocks, U.F., and H. Chandra (1982). *Acta Metall.*, 30, 695-709.

Kocks, U.F., P. Franciosi, and M. Kawai (1988). In preparation.

Matthies, S., and H.-R. Wenk (1981). In H.-R. Wenk (Ed.), *Preferred Orientation in Deformed Metals and Rocks*. Academic Press. pp. 139-147.

Mecking, H. (1981). In N. Hansen et.al.(Eds.), *Deformation of Polycrystals*. Risø National Laboratory, Roskilde, Denmark. pp. 73-86.

Mecking, H., B. Nicklas, N. Zarubová and U.F. Kocks (1986). *Acta Metall.* 8, 527-535.

Stout, M.G., J.S. Kallend, U.F. Kocks, M.A. Przystupa and A.D. Rollett (1987). In J.S. Kallend and G. Gottstein (Eds.), *Eighth Int'l. Conf. on Textures of Materials*. The Metallurgical Society, Warrendale, Pa. In press.

Tomé, C., G.R. Canova, U.F. Kocks, N. Christodoulou and J.J. Jonas (1984). *Acta Metall.*, 32, 1637-1653.

Wenk, H.-R. (1985). In H.-R. Wenk (Ed.), *Preferred Orientation in Deformed Metals and Rocks*. Academic Press. pp.11-47.